

Thermal buckling of functionally graded plates using a n-order four variable refined theory

Z. Abdelhak^{*1}, L. Hadji^{1,2}, T.H. Daouadji^{1,2} and E.A Bedia²

¹Université Ibn Khaldoun, BP 78 Zaaroura, 14000 Tiaret, Algérie.

²Laboratoire des Matériaux & Hydrologie, Université de Sidi Bel Abbès, 22000 Sidi Bel Abbès, Algérie.

(Received December 2, 2014, Revised January 28, 2015, Accepted February 25, 2015)

Abstract. This paper presents a simple n-order four variable refined theory for buckling analysis of functionally graded plates. By dividing the transverse displacement into bending and shear parts, the number of unknowns and governing equations of the present theory is reduced, and hence, makes it simple to use. The present theory is variationally consistent, uses the n-order polynomial term to represent the displacement field, does not require shear correction factor, and eliminates the shear stresses at the top and bottom surfaces. A power law distribution is used to describe the variation of volume fraction of material compositions. Equilibrium and stability equations are derived based on the present n-order refined theory. The non-linear governing equations are solved for plates subjected to simply supported boundary conditions. The thermal loads are assumed to be uniform, linear and non-linear distribution through-the-thickness. The effects of aspect and thickness ratios, gradient index, on the critical buckling are all discussed.

Keywords: nth-order four variable refined theory; functionally graded plates; thermal buckling

1. Introduction

Functionally graded materials (FGMs) are new inhomogeneous materials which have widely used in many engineering applicants such as nuclear reactors and high-speed spacecraft industries (Yamanouchi *et al.* 1990). The mechanical properties of FGMs vary smoothly and continuously from one surface to the other. Typically these materials are made from a mixture of ceramic and metal or from a combination of different materials. The ceramic constituent of the material provides the high-temperature resistance due to its low thermal conductivity. The ductile metal constituent on the other hand, prevents fracture caused by stresses due to the high temperature gradient in a very short period of time. Furthermore a mixture of ceramic and metal with a continuously varying volume fraction can be easily manufactured (Fukui 1991, Koizumi 1997). With the developments in manufacturing methods (Fukui *et al.* 1991, Fukui *et al.* 1997 and El-Hadek *et al.* 2003) functionally graded materials seem to have great potential in sandwich structures. The analysis of these materials has been considered by many researchers. The functionally graded (FG) plates are commonly used in thermal environments; they can buckle under thermal and mechanical loads. Thus, the buckling analysis of such plates is essential to

*Corresponding Author, Professor, E-mail: had_laz@yahoo.fr

ensure an efficient and reliable design. Eslami and his co-workers (Javaheri *et al.* 2002, Samsam *et al.* 2005) have treated a series of problems relating to the linear buckling of simply supported rectangular FG plates, with and without imperfections, under mechanical and thermal loads. By using an analytical approach, they obtained closed-form expressions for buckling loads. Sohn *et al.* (2008) dealt with the stabilities of FG panels subjected to combined thermal and aerodynamic loads. The first-order theory was used to simulate supersonic aerodynamic loads acting on the panels. The influence of the material constitution of FG panels on thermal buckling and flutter characteristics was examined. Zenkour *et al.* (2010a) studied the thermal Buckling Analysis of Ceramic-Metal Functionally Graded Plates. Bouiadjra *et al.* (2012) developed a four-variable refined plate theory for buckling analysis of functionally graded plates. Song *et al.* (2013) used a n -order four variable refined theory for bending and free vibration of functionally graded plates. Klouche (2014) studied the bending and free vibration of functionally graded plates by using a n -order four variable refined theory. The n -order four variable refined theory proposed by Song *et al.* (2013) is based on the assumption that the in-plane and transverse displacements consist of bending and shear components in which the bending components do not contribute toward shear forces and, likewise, the shear components do not contribute toward bending moments.

The most interesting feature of this theory is uses the n -order polynomial term to represent the displacement field, does not require shear correction factor, and eliminates the shear stresses at the top and bottom surfaces. Although several studies on the buckling of FG plates have been carried out based on variety of plate theories, no studies can be found for the thermal buckling of FG plates based on the refined theory proposed by Song Xiang *et al.* (2013). Therefore, the aim of this study is to extend the n -order refined theory to the thermal buckling of FG plates. The material properties of FG plate are assumed to vary according to a power law distribution of the volume fraction of the constituents. The n -order four variable refined theory is used to obtain the buckling of the plate under different types of thermal loads. The thermal loads are assumed to be uniform, linear and non-linear distribution through the thickness. Illustrative examples are given so as to demonstrate the efficacies of the theory. The effects of various variables, such as thickness and aspect ratios, gradient index, on the critical buckling are all discussed.

2. Theoretical formulation

2.1 Displacement field and strains

Consider a plate of total thickness h and composed of functionally graded material through the thickness. It is assumed that the material is isotropic and grading is assumed to be only through the thickness. The xy plane is taken to be the undeformed mid plane of the plate with the z axis positive upward from the mid plane. The displacement field of this theory is as follows:

$$\begin{aligned} u(x, y, z, t) &= u_0(x, y, t) - z \frac{\partial w_b}{\partial x} - \frac{1}{n} \left(\frac{2}{h} \right)^{n-1} z^n \frac{\partial w_s}{\partial x} \\ v(x, y, z, t) &= v_0(x, y, t) - z \frac{\partial w_b}{\partial y} - \frac{1}{n} \left(\frac{2}{h} \right)^{n-1} z^n \frac{\partial w_s}{\partial y} \end{aligned} \quad (1)$$

$$n = 3, 5, 7, 9, \dots$$

$$w(x, y, z, t) = w_b(x, y, t) + w_s(x, y, t)$$

where u_0 and v_0 are the mid-plane displacements of the plate in the x and y direction, respectively; w_b and w_s are the bending and shear components of transverse displacement, respectively.

The non-linear von Karman strain–displacement equations are as follows:

$$\begin{Bmatrix} \varepsilon_x \\ \varepsilon_y \\ \gamma_{xy} \end{Bmatrix} = \begin{Bmatrix} \varepsilon_x^0 \\ \varepsilon_y^0 \\ \gamma_{xy}^0 \end{Bmatrix} + z \begin{Bmatrix} k_x^b \\ k_y^b \\ k_{xy}^b \end{Bmatrix} + f(z) \begin{Bmatrix} k_x^s \\ k_y^s \\ k_{xy}^s \end{Bmatrix}, \quad \begin{Bmatrix} \gamma_{yz} \\ \gamma_{xz} \end{Bmatrix} = g(z) \begin{Bmatrix} \gamma_{yz}^s \\ \gamma_{xz}^s \end{Bmatrix}, \quad \varepsilon_z = 0 \quad (2)$$

where

$$\begin{Bmatrix} \varepsilon_x^0 \\ \varepsilon_y^0 \\ \gamma_{xy}^0 \end{Bmatrix} = \begin{Bmatrix} \frac{\partial u_0}{\partial x} + \frac{1}{2} \left(\frac{\partial w_b}{\partial x} + \frac{\partial w_s}{\partial x} \right)^2 \\ \frac{\partial v_0}{\partial y} + \frac{1}{2} \left(\frac{\partial w_b}{\partial y} + \frac{\partial w_s}{\partial y} \right)^2 \\ \frac{\partial u_0}{\partial y} + \frac{\partial v_0}{\partial x} + \left(\frac{\partial w_b}{\partial x} + \frac{\partial w_s}{\partial x} \right) \left(\frac{\partial w_b}{\partial y} + \frac{\partial w_s}{\partial y} \right) \end{Bmatrix}, \quad \begin{Bmatrix} k_x^b \\ k_y^b \\ k_{xy}^b \end{Bmatrix} = \begin{Bmatrix} -\frac{\partial^2 w_b}{\partial x^2} \\ -\frac{\partial^2 w_b}{\partial y^2} \\ -2\frac{\partial^2 w_b}{\partial x \partial y} \end{Bmatrix} \quad (3)$$

$$\begin{Bmatrix} k_x^s \\ k_y^s \\ k_{xy}^s \end{Bmatrix} = \begin{Bmatrix} -\frac{\partial^2 w_s}{\partial x^2} \\ -\frac{\partial^2 w_s}{\partial y^2} \\ -2\frac{\partial^2 w_s}{\partial x \partial y} \end{Bmatrix}, \quad \begin{Bmatrix} \gamma_{yz}^s \\ \gamma_{xz}^s \end{Bmatrix} = \begin{Bmatrix} \frac{\partial w_s}{\partial y} \\ \frac{\partial w_s}{\partial x} \end{Bmatrix}$$

$$f(z) = \frac{z^n}{n} \left(\frac{2}{h} \right)^{n-1}; \quad \text{and} \quad g(z) = 1 - \frac{df(z)}{dz} = 1 - \frac{z^n}{z} \left(\frac{2}{h} \right)^{n-1}$$

2.2 Constitutive relations

Consider a functionally graded plate, which is made from a mixture of ceramics and metals. The plate is subjected to a thermal load $T(x, y, z)$. It is assumed that the composition properties of FGM vary through the thickness of the plate.

The variation of material properties can be expressed as :

$$P(z) = P_b + (P_t - P_b)V_t \quad (4)$$

where P denotes a generic material property like modulus and P_t and P_b denote the corresponding properties of the top and bottom faces of the plate, respectively. Also V_t in Eq. (4) denotes the volume fraction of the top face constituent and follows a simple power-law as:

$$V_t = \left(\frac{z}{h} + \frac{1}{2} \right)^k \quad (5)$$

where k ($0 \leq k \leq \infty$) is a parameter that dictates the material variation profile through the thickness. Here we assume that moduli E , G and the coefficient of thermal expansion α vary according to Eq. (4) and the Poisson's ratio ν is assumed to be a constant.

The linear constitutive relations are :

$$\begin{Bmatrix} \sigma_x \\ \sigma_y \\ \tau_{xy} \end{Bmatrix} = \begin{bmatrix} Q_{11} & Q_{12} & 0 \\ Q_{12} & Q_{22} & 0 \\ 0 & 0 & Q_{66} \end{bmatrix} \begin{Bmatrix} \varepsilon_x - \alpha T \\ \varepsilon_y - \alpha T \\ \gamma_{xy} \end{Bmatrix} \quad \text{and} \quad \begin{Bmatrix} \tau_{yz} \\ \tau_{zx} \end{Bmatrix} = \begin{bmatrix} Q_{44} & 0 \\ 0 & Q_{55} \end{bmatrix} \begin{Bmatrix} \gamma_{yz} \\ \gamma_{zx} \end{Bmatrix} \quad (6)$$

where $(\sigma_x, \sigma_y, \tau_{xy}, \tau_{xz}, \tau_{yz})$ and $(\varepsilon_x, \varepsilon_y, \gamma_{xy}, \gamma_{xz}, \gamma_{yz})$ are the stress and strain components, respectively. Using the material properties defined in Eq. (4), stiffness coefficients, Q_{ij} , can be expressed as

$$Q_{11} = Q_{22} = \frac{E(z)}{1-\nu^2} \quad (7a)$$

$$Q_{12} = \frac{\nu E(z)}{1-\nu^2} \quad (7b)$$

$$Q_{44} = Q_{55} = Q_{66} = \frac{E(z)}{2(1+\nu)} \quad (7c)$$

2.3 Stability equations

The total potential energy of the FG plate may be written as

$$U = \frac{1}{2} \iiint \left[\sigma_x (\varepsilon_x - \alpha T) + \sigma_y (\varepsilon_y - \alpha T) + \tau_{xy} \gamma_{xy} + \tau_{yz} \gamma_{yz} + \tau_{xz} \gamma_{xz} \right] dx dy dz \quad (8)$$

The principle of virtual work for the present problem may be expressed as follows :

$$\iint \left[N_x \delta \varepsilon_x^0 + N_y \delta \varepsilon_y^0 + N_{xy} \delta \gamma_{xy}^0 + M_x^b \delta k_x^b + M_y^b \delta k_y^b + M_{xy}^b \delta k_{xy}^b + M_x^s \delta k_x^s \right. \\ \left. + M_y^s \delta k_y^s + M_{xy}^s \delta k_{xy}^s + S_{yz}^s \delta \gamma_{yz}^s + S_{xz}^s \delta \gamma_{xz}^s \right] dx dy = 0 \quad (9)$$

where

$$\begin{Bmatrix} N_x & N_y & N_{xy} \\ M_x^b & M_y^b & M_{xy}^b \\ M_x^s & M_y^s & M_{xy}^s \end{Bmatrix} = \int_{-h/2}^{h/2} \left(\sigma_x, \sigma_y, \tau_{xy} \right) \begin{Bmatrix} 1 \\ z \\ f(z) \end{Bmatrix} dz \quad (10a)$$

$$\left(S_{xz}^s, S_{yz}^s \right) = \int_{-h/2}^{h/2} (\tau_{xz}, \tau_{yz}) g(z) dz. \quad (10b)$$

Using Eq. (6) in Eq. (10), the stress resultants of the FG plate can be related to the total strains by

$$\begin{Bmatrix} N \\ M^b \\ M^s \end{Bmatrix} = \begin{bmatrix} A & B & B^s \\ B & D & D^s \\ B^s & D^s & H^s \end{bmatrix} \begin{Bmatrix} \varepsilon \\ k^b \\ k^s \end{Bmatrix} - \begin{Bmatrix} N^T \\ M^{bT} \\ M^{sT} \end{Bmatrix}, \quad S = A^s \gamma \quad (11)$$

where

$$N = \{N_x, N_y, N_{xy}\}^t, \quad M^b = \{M_x^b, M_y^b, M_{xy}^b\}^t, \quad M^s = \{M_x^s, M_y^s, M_{xy}^s\}^t \quad (12a)$$

$$N^T = \{N_x^T, N_y^T, 0\}^t, \quad M^{bT} = \{M_x^{bT}, M_y^{bT}, 0\}^t, \quad M^{sT} = \{M_x^{sT}, M_y^{sT}, 0\}^t \quad (12b)$$

$$\varepsilon = \{\varepsilon_x^0, \varepsilon_y^0, \gamma_{xy}^0\}^t, \quad k^b = \{k_x^b, k_y^b, k_{xy}^b\}^t, \quad k^s = \{k_x^s, k_y^s, k_{xy}^s\}^t \quad (12c)$$

$$A = \begin{bmatrix} A_{11} & A_{12} & 0 \\ A_{12} & A_{22} & 0 \\ 0 & 0 & A_{66} \end{bmatrix}, \quad B = \begin{bmatrix} B_{11} & B_{12} & 0 \\ B_{12} & B_{22} & 0 \\ 0 & 0 & B_{66} \end{bmatrix}, \quad D = \begin{bmatrix} D_{11} & D_{12} & 0 \\ D_{12} & D_{22} & 0 \\ 0 & 0 & D_{66} \end{bmatrix} \quad (12d)$$

$$B^s = \begin{bmatrix} B_{11}^s & B_{12}^s & 0 \\ B_{12}^s & B_{22}^s & 0 \\ 0 & 0 & B_{66}^s \end{bmatrix}, \quad D^s = \begin{bmatrix} D_{11}^s & D_{12}^s & 0 \\ D_{12}^s & D_{22}^s & 0 \\ 0 & 0 & D_{66}^s \end{bmatrix}, \quad H^s = \begin{bmatrix} H_{11}^s & H_{12}^s & 0 \\ H_{12}^s & H_{22}^s & 0 \\ 0 & 0 & H_{66}^s \end{bmatrix} \quad (12e)$$

$$S = \{S_{xz}^s, S_{yz}^s\}^t, \quad \gamma = \{\gamma_{xz}^s, \gamma_{yz}^s\}^t, \quad A^s = \begin{bmatrix} A_{44}^s & 0 \\ 0 & A_{55}^s \end{bmatrix} \quad (12f)$$

where A_{ij} , B_{ij} , etc., are the plate stiffness, defined by

$$\begin{Bmatrix} A_{11} & B_{11} & D_{11} & B_{11}^s & D_{11}^s & H_{11}^s \\ A_{12} & B_{12} & D_{12} & B_{12}^s & D_{12}^s & H_{12}^s \\ A_{66} & B_{66} & D_{66} & B_{66}^s & D_{66}^s & H_{66}^s \end{Bmatrix} = \int_{-h/2}^{h/2} \left(1, z, z^2, f(z), zf(z), f^2(z) \right) \begin{Bmatrix} 1 \\ \nu^{(n)} \\ \frac{1-\nu^{(n)}}{2} \end{Bmatrix} dz \quad (13a)$$

and

$$(A_{22}, B_{22}, D_{22}, B_{22}^s, D_{22}^s, H_{22}^s) = (A_{11}, B_{11}, D_{11}, B_{11}^s, D_{11}^s, H_{11}^s) \quad (13b)$$

$$A_{44}^s = A_{55}^s = \int_{-h/2}^{h/2} \frac{E(z)}{2(1-\nu)} [g(z)]^2 dz \quad (13c)$$

The stress and moment resultants, $N_x^T = N_y^T$, $M_x^{bT} = M_y^{bT}$ and $M_x^{sT} = M_y^{sT}$ due to thermal loading are defined by

$$\begin{Bmatrix} N_x^T \\ M_x^{bT} \\ M_x^{sT} \end{Bmatrix} = \int_{-h/2}^{h/2} \frac{E(z)}{1-\nu} \alpha(z) T \begin{Bmatrix} 1 \\ z \\ f(z) \end{Bmatrix} dz \quad (14)$$

The stability equations of the plate may be derived by the adjacent equilibrium criterion. Assume that the equilibrium state of the FG plate under thermal loads is defined in terms of the displacement components $(u_0^0, v_0^0, w_b^0, w_s^0)$. The displacement components of a neighboring stable state differ by $(u_0^1, v_0^1, w_b^1, w_s^1)$ with respect to the equilibrium position. Thus, the total displacements of a neighboring state are

$$u_0 = u_0^0 + u_0^1, \quad v_0 = v_0^0 + v_0^1, \quad w_b = w_b^0 + w_b^1, \quad w_s = w_s^0 + w_s^1, \quad (15)$$

where the superscript 1 refers to the state of stability and the superscript 0 refers to the state of equilibrium conditions.

Substituting Eqs. (2) and (15) into Eq. (9) and integrating by parts and then equating the coefficients of δu_0^1 , δv_0^1 , δw_b^1 , δw_s^1 , to zero, separately, the governing stability equations are obtained for the shear deformation plate theories as

$$\begin{aligned} \frac{\partial N_x^1}{\partial x} + \frac{\partial N_{xy}^1}{\partial y} &= 0 \\ \frac{\partial N_{xy}^1}{\partial x} + \frac{\partial N_y^1}{\partial y} &= 0 \\ \frac{\partial^2 M_x^{b1}}{\partial x^2} + 2 \frac{\partial^2 M_{xy}^{b1}}{\partial x \partial y} + \frac{\partial^2 M_y^{b1}}{\partial y^2} + \bar{N} &= 0 \\ \frac{\partial^2 M_x^{s1}}{\partial x^2} + 2 \frac{\partial^2 M_{xy}^{s1}}{\partial x \partial y} + \frac{\partial^2 M_y^{s1}}{\partial y^2} + \frac{\partial S_{xz}^{s1}}{\partial x} + \frac{\partial S_{yz}^{s1}}{\partial y} + \bar{N} &= 0 \end{aligned} \quad (16)$$

with

$$\bar{N} = \left[N_x^0 \frac{\partial^2 (w_b^1 + w_s^1)}{\partial x^2} + N_y^0 \frac{\partial^2 (w_b^1 + w_s^1)}{\partial y^2} + 2N_{xy}^0 \frac{\partial^2 (w_b^1 + w_s^1)}{\partial x \partial y} \right] \quad (17)$$

where the terms N_x^0 and N_y^0 are the pre-buckling force resultants obtained as

$$N_x^0 = N_y^0 = - \int_{-h/2}^{h/2} \frac{\alpha(z)E(z)T}{1-\nu} dz. \quad (18)$$

3. Exact solution for a simply-supported fgm plate

Rectangular plates are generally classified in accordance with the type of support used. We are here concerned with the exact solution of Eqs. (16) for a simply supported FG plate. The following boundary conditions are imposed at the side edges for the present four variable refined plate theory :

$$v_0^1 = w_b^1 = w_s^1 = \frac{\partial w_s^1}{\partial y} = N_x^1 = M_x^{b1} = M_x^{s1} = 0 \quad \text{at } x=0, a, \quad (19a)$$

$$u_0^1 = w_b^1 = w_s^1 = \frac{\partial w_s^1}{\partial x} = N_y^1 = M_y^{b1} = M_y^{s1} = 0 \quad \text{at } y=0, b. \quad (19b)$$

The following approximate solution is seen to satisfy both the differential equation and the boundary conditions

$$\begin{Bmatrix} u_0^1 \\ v_0^1 \\ w_b^1 \\ w_s^1 \end{Bmatrix} = \sum_{m=1}^{\infty} \sum_{n=1}^{\infty} \begin{Bmatrix} U_{mn}^1 \cos(\lambda x) \sin(\mu y) \\ V_{mn}^1 \sin(\lambda x) \cos(\mu y) \\ W_{bmn}^1 \sin(\lambda x) \sin(\mu y) \\ W_{smn}^1 \sin(\lambda x) \sin(\mu y) \end{Bmatrix} \quad (20)$$

where U_{mn}^1 , V_{mn}^1 , W_{bmn}^1 and W_{smn}^1 are arbitrary parameters to be determined, $\lambda = m\pi/a$ and $\mu = n\pi/b$ and m and n are mode numbers. Substituting Eq. (20) into Eq. (16), one obtains

$$[K]\{\Delta\} = \{P\} \quad (21)$$

where $\{\Delta\}$ denotes the column

$$\{\Delta\} = \{U_{mn}^1, V_{mn}^1, W_{bmn}^1, W_{smn}^1\}^t \quad (22)$$

and $[K]$ is the symmetric matrix given by

$$[K] = \begin{bmatrix} a_{11} & a_{12} & a_{13} & a_{14} \\ a_{12} & a_{22} & a_{23} & a_{24} \\ a_{13} & a_{23} & a_{33} & a_{34} \\ a_{14} & a_{24} & a_{34} & a_{44} \end{bmatrix} \quad (23)$$

For nontrivial solution, the determinant of the coefficient matrix in Eq. (21) must be zero. This gives the thermal buckling load.

3.1 Buckling of FG Plates under Uniform Temperature Rise

The plate initial temperature is assumed to be T_i . The temperature is uniformly raised to a final value T_f in which the plate buckles. The temperature change is $\Delta T = T_f - T_i$.

3.2 Buckling of FG Plates Subjected to Graded Temperature Change Across the Thickness

We assume that the temperature of the top surface is T_t and the temperature varies from T_t according to the power law variation through-the-thickness, to the bottom surface temperature T_b in which the plate buckles. In this case, the temperature through-the-thickness is given by

$$T(z) = \Delta T \left(\frac{z}{h} + \frac{1}{2} \right)^\gamma + T_t \quad (24)$$

where the buckling temperature difference $\Delta T = T_t - T_b$ and γ is the temperature exponent ($0 < \gamma < \infty$). Note that the value of γ equal to unity represents a linear temperature change across the thickness. While the value of γ excluding unity represents a non-linear temperature change through-the-thickness.

4. Numerical results

In this section, various numerical examples are presented and discussed for verifying the accuracy and efficiency of the present theory in predicting the critical buckling temperature change of simply supported FG plates under uniform, linear and nonlinear thermal loading through the thickness. For the verification purpose, the results obtained by the present four variable refined plate theory are compared with the existing data in the literature.

It is assumed that the functionally graded plate is made of a mixture of aluminum and alumina. The Young modulus, coefficient of thermal expansion and thermal conductivity for aluminum are $E_m = 70GPa$, $\alpha_m = 23.10^{-6} / ^\circ C$, and for alumina are $E_c = 380GPa$, $\alpha_c = 7.4 \times 10^{-6} / ^\circ C$ respectively.

In order to prove the validity of the present formulation, results were obtained for FG plates under uniform, linear and nonlinear thermal loading through the thickness according to all theories.

In Tables 1 and 2 the results of buckling analysis for the plate under uniform temperature rise are presented. These tables show the comparisons of the critical buckling temperature change obtained by the present theory with those given by [Javaheri et al. \(2002\)](#) based on both higher plate theory (HPT) and the classical plate theory (CPT), and [Zenkour and Mashat \(2010\)](#) based on sinusoidal plate theory (SPT). The results of the present theory show very good agreement with HPT and SPT both for thin and thick FG plates.

Table 1 show that the buckling temperature increases by the increase of the aspect ratio a/b and decreases with increase of the power law index (k) from 0 to 10. Table 2 shows that the buckling temperature decreases by the increase of the dimension ratio a/h and the power law

Table 1 Critical buckling temperature of FG plate under uniform temperature rise for different values of power law index k and aspect ratio a/b with $a/b = 100$

k	Theory	a/b=1	a/b=2	a/b=3	a/b=4	a/b=5
0	Present (n=3)	17.0894	42.6875	85.2551	144.6490	220.6706
	Present (n=5)	17.0896	42.6888	85.2600	144.6630	220.7033
	Present (n=7)	17.0898	42.6902	85.2658	144.6798	220.7423
	Present (n=9)	17.0900	42.6913	85.2703	144.6927	220.7723
	HPT*	17.08	42.68	85.25	144.64	220.66
	SPT [#]	17.08	42.68	85.25	144.65	220.28
	CPT*	17.09	42.74	85.49	145.34	222.28
1	Present (n=3)	7.9400	19.8358	39.6248	67.2506	102.6356
	Present (n=5)	7.9400	19.8363	39.6267	67.2561	102.6484
	Present (n=7)	7.9401	19.8369	39.6289	67.2627	102.6637
	Present (n=9)	7.9402	19.8373	39.6307	67.2678	102.6754
	HPT*	7.94	19.83	39.62	67.25	102.63
	SPT [#]	7.94	19.83	39.62	67.25	102.63
	CPT*	7.94	19.83	39.71	67.52	103.26
5	Present (n=3)	7.2606	18.1327	36.2025	61.3951	93.6069
	Present (n=5)	7.2609	18.1346	36.2102	61.4174	93.6585
	Present (n=7)	7.2612	18.1361	36.2161	61.4344	93.6981
	Present (n=9)	7.2613	18.1371	36.2202	61.4463	93.7258
	HPT*	7.26	18.13	36.20	61.39	93.60
	SPT [#]	7.26	18.13	36.20	61.39	93.60
	CPT*	7.26	18.13	36.20	61.75	94.45
10	Present (n=3)	7.4634	18.6366	37.2006	63.0687	96.1213
	Present (n=5)	7.4636	18.6382	37.2069	63.0870	96.1638
	Present (n=7)	7.4639	18.6398	37.2131	63.1047	96.2050
	Present (n=9)	7.4641	18.6409	37.2178	63.1182	96.2363
	HPT*	7.46	18.63	37.20	63.06	96.12
	SPT [#]	7.46	18.63	37.20	63.06	96.11
	CPT*	7.46	18.67	37.34	63.48	97.10

[#] Results form Ref (Zenkour et al. 2010)

* Results form Ref (Javaheri et al. 2002b)

Table 2 Critical buckling temperature of square FG plate under uniform temperature rise for different values of power law index k and side-to-thickness ratio a/h

k	Theory	a/h=10	a/h=20	a/h=40	a/h=60	a/h=80	a/h=100
0	Present (n=3)	1618.6819	421.5352	106.4940	47.4232	26.6938	17.0894
	Present (n=5)	1620.4093	421.6542	106.5016	47.4247	26.6943	17.0896
	Present (n=7)	1622.5030	421.7964	106.5107	47.4265	26.6948	17.0898
	Present (n=9)	1624.1224	421.9060	106.5177	47.4279	26.6953	17.0900
	HPT*	1617.48	421.52	106.49	47.42	26.69	17.08
	CPT*	1709.91	427.47	106.87	47.49	26.71	17.09

Table 2 Critical buckling temperature of square FG plate under uniform temperature rise for different values of power law index k and side-to-thickness ratio a/h

k	Theory	$a/h=10$	$a/h=20$	$a/h=40$	$a/h=60$	$a/h=80$	$a/h=100$
1	Present (n=3)	758.3956	196.2652	49.5016	22.0369	12.4029	7.9400
	Present (n=5)	759.0826	196.3119	49.5046	22.0375	12.4031	7.9400
	Present (n=7)	759.9150	196.3678	49.5082	22.0382	12.4033	7.9401
	Present (n=9)	760.5586	196.4108	49.5109	22.0388	12.4035	7.9402
	HPT*	757.89	196.26	49.50	22.03	12.40	7.94
	CPT*	794.37	198.59	49.64	22.06	12.41	7.94
5	Present (n=3)	697.3104	178.5353	45.2139	20.1435	11.3403	7.2606
	Present (n=5)	682.0146	178.7230	45.2259	20.1459	11.3410	7.2609
	Present (n=7)	684.1093	178.8669	45.2352	20.1477	11.3416	7.2612
	Present (n=9)	685.5860	178.9679	45.2416	20.1490	11.3420	7.2613
	HPT*	678.92	178.53	45.21	20.14	11.34	7.26
	CPT*	726.57	181.64	45.41	20.18	11.35	7.26
10	Present (n=3)	692.6947	183.1444	46.4554	20.7029	11.6564	7.4634
	Present (n=5)	694.8769	183.2983	46.4653	20.7048	11.6570	7.4636
	Present (n=7)	697.0254	183.4480	46.4749	20.7067	11.6576	7.4639
	Present (n=9)	698.6695	183.5618	46.4822	20.7082	11.6581	7.4641
	HPT*	692.52	183.14	46.45	20.70	11.65	7.46
	CPT*	746.92	186.73	46.68	20.74	11.67	7.46

* Results form Ref (Javaheri et al. 2002)

Results form Ref (Zenkour et al. 2010)

index (k) from 0 to 10. It is interesting to note that the buckling temperatures for homogeneous plates ($k = 0$) are considerably higher than those for the FG plates ($k > 0$), especially for the comparatively longer and thicker plates. The critical buckling temperatures obtained based on classical plate theory are noticeably greater than values obtained based on higher order shear deformation theory. The differences are considerable for long and thin plates.

In Tables 3 and 4 the results of buckling analysis for the plate under linear temperature change across the thickness are presented. It can be seen that the results of present theory are almost identical with those reported by Javaheri and Eslami (2002) based on HPT and by Zenkour and Mashat (2010) based on SPT. It is concluded that the buckling temperature increases by the increase of the aspect ratio a/b , decreases by the increase of the power law index (k) and decreases by the increase of the dimension ratio a/h .

Also, the buckling temperatures for homogeneous plates are considerably higher than those for the FG plates especially for the comparatively longer and thicker plates. The critical buckling temperatures obtained based on classical plate theory are noticeably greater than values obtained based on higher order shear deformation theory. The differences are considerable for long and thin plates. Hence, in order to obtain accurate results for thick FG plates, it is necessary to consider the transverse shear deformation effects by using shear deformation theories. It should be noted that the unknown function in present theory is only four, while the unknown function in both HPT and SPT is five. It can be concluded that the present theory is not only accurate but also simple in predicting critical buckling temperature of FG plates.

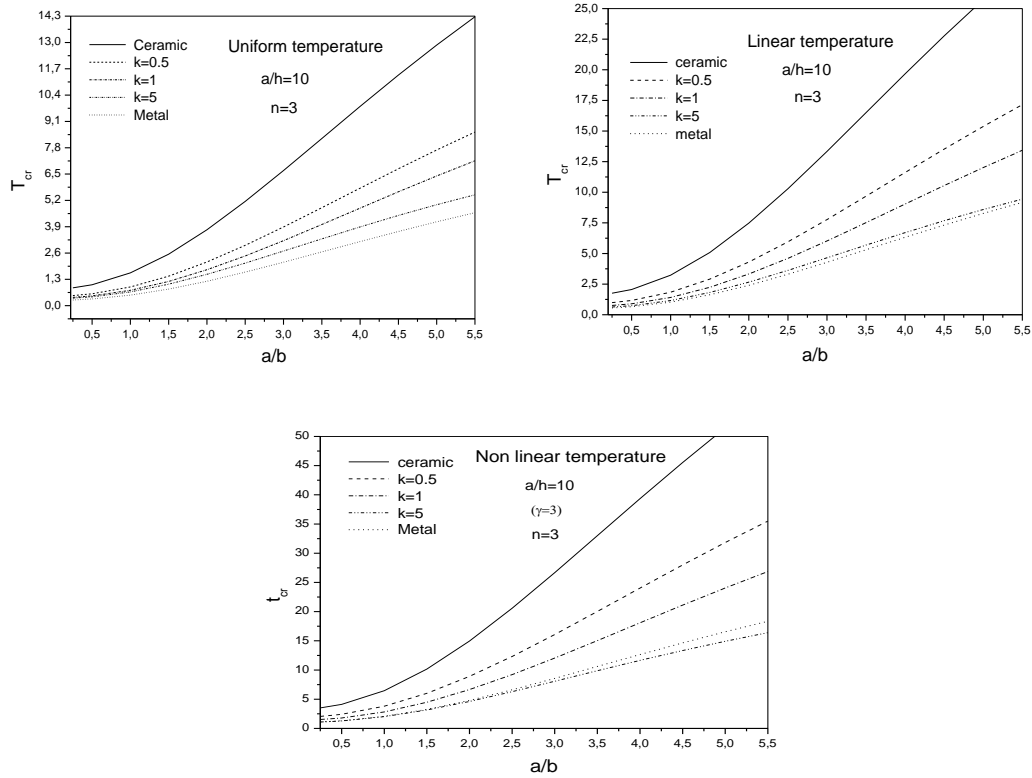


Fig. 1 Critical buckling temperature difference T_{cr} due to uniform, linear and non-linear temperature rise across the thickness versus the aspect ratio a/b ($n=3$)

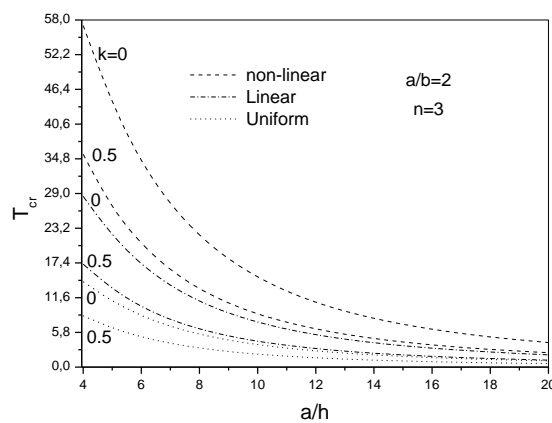


Fig. 2 Critical buckling temperature difference T_{cr} due to uniform, linear and non-linear temperature rise across the thickness versus the side-to-thickness ratio a/h ($n=3$)

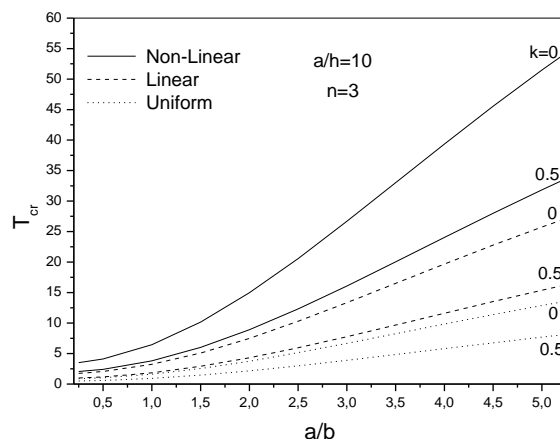


Fig. 3 Critical buckling temperature difference T_{cr} due to uniform, linear and non-linear temperature rise across the thickness versus the aspect ratio a/b ($n=3$).

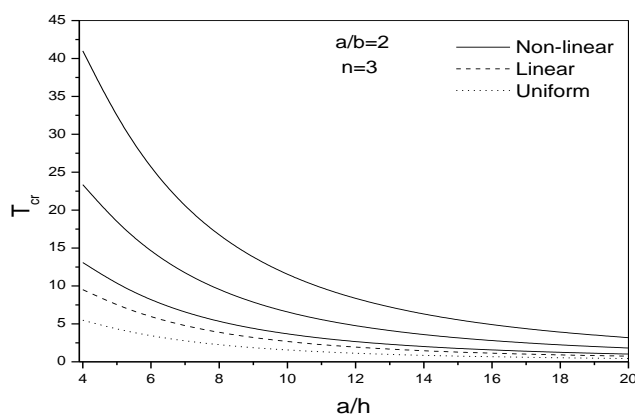


Fig. 4 Critical buckling temperature difference T_{cr} due to uniform, linear and non-linear temperature rise across the thickness versus the side-to-thickness ratio a/h and for different values of the nonlinearity parameter γ ($k=5, n=3$)

Tables 5 exhibit the critical temperature difference $t_{cr} = 10^{-3}T_{cr}$ for different values of the aspect ratio a/b , the temperature exponent γ and the power law index k under non-linear temperature loads at $a/h=10$. The nonlinearity temperature exponent γ is taken here as 2, 5 and 10. It can be concluded from the presented results that the present theory gives more accurate results of critical buckling temperature when compared to the higher-order shear deformation theory.

The effect of a/b on the critical buckling t_{cr} is similar to that in the case of uniform and linear temperature difference across the thickness. As the power law index k increases, the critical buckling t_{cr} decreases to reach lowest values and then increases excluding t_{cr} of the rectangular plates for $\gamma=10$. It is also noticed from Table 5 that the t_{cr} increases with the increase of the non-linearity parameter γ .

In general, the values of the critical temperature difference calculated by using the shear deformation theories are lower than those calculated by using the classical plate theory, indicating the shear deformation effect.

Figure 1 shows the variation trend of critical temperature difference t_{cr} with respect to the plate aspect ratio a/b for different values of material gradient index k under a uniform, linear and non-linear temperature loads. It is observed that with increasing the plate aspect ratio a/b , the critical buckling temperature difference also increases steadily, whatever the material gradient index k is. Because the ceramic plate is weaker than the metallic one, thus the critical buckling temperature of the first plate is higher than that of the second. For the FG plate, t_{cr} decreases as the metallic constituent in the plate increases.

The critical buckling temperature change t_{cr} versus the side-to-thickness ratio a/h and the aspect ratio a/b of FG plates under various thermal loading types is exhibited in Figures 2–4.

It can be seen from these figures that, regardless of the loading type and the power-law index k , the critical buckling temperature difference t_{cr} decreases as the side-to-thickness ratio a/h increases and it is reduced with the decrease of the aspect ratio a/b . The critical buckling temperature for the ceramic plate is higher than that for the FG plate. This is because the ceramic plate is stronger than the other. The differences between the loading types decrease with the increase of a/h because the plate becomes thin. It is also noticed from figure 4 that the t_{cr} increases with the increase of the non-linearity parameter γ .

5. Conclusion

This paper presents a simple n-order four variable refined theory for buckling analysis of functionally graded plates. The present theory is variationally consistent, uses the n-order polynomial term to represent the displacement field, does not require shear correction factor, and eliminates the shear stresses at the top and bottom surfaces. A power law distribution is used to describe the variation of volume fraction of material compositions.

Equilibrium and stability equations are derived based on the present n-order refined theory. The non-linear governing equations are solved for plates subjected to simply supported boundary conditions. The thermal loads are assumed to be uniform, linear and non-linear distribution through-the-thickness.

Based on the above discussion, some conclusions are listed as follows :

- It is shown through the numerical examples that the present theory can provide accurate results for critical temperatures of FG plates subjected to uniformly, linearly and non-linearly distributed temperatures across the thickness.
- The critical buckling temperature difference of FG plates decreases when the side to-

thickness ratio increases a/h .

- The critical buckling temperature difference t_{cr} for FG plates is increased by increasing the aspect ratio a/b .
- The higher order shear deformation theory underestimates the buckling load compared with the classical plate theory.
- The critical buckling temperature of FG plate under non-linear temperature rise across the thickness increases as the temperature exponent γ increases.

References

- Bouiadjra, M.B., Sid Ahmed, M.H. and Abdelouahed Tounsi, A. (2012), "Thermal buckling of functionally graded plates according to a four-variable refined plate theory", *J. Thermal Stresses*, **35**, 677-694.
- El-Hadek, M. and Tippur, H.V. (2003), "Dynamic fracture parameters and constraint effects in functionally graded syntactic epoxy foams", *Int. J. Solids Struct.*, **40**, 1885-1906.
- Fukui, Y. (1991), "Fundamental investigation of functionally gradient material manufacturing system using centrifugal force", *Int. J. Japanese Soci. Mech. Eng.*, **3**, 144-148.
- Fukui, Y., Yamanaka, N. and Enokida, Y. (1997), "Bending strength of an Al-Al₃Ni functionally graded material", *Composites: Part B*, **28B**, 37-43.
- Javaheri, R. and Eslami, M.R. (2002a), "Buckling of functionally graded plates under in-plane compressive loading", *ZAMM*, **82**(4), 277-283.
- Javaheri, R. and Eslami, M.R. (2002b), "Thermal buckling of functionally graded plates", *AIAA*, **40**(1), 162-169.
- Javaheri, R. and Eslami, M.R. (2002) "Thermal buckling of functionally graded plates based on higher order theory", *J. Therm. Stress.*, **25**(1), 603-625.
- Klouche Djedid, I., Benachour, A., Houari, M.S.A., Tounsi, A. and Ameer, M. (2014), "An-order four variable refined theory for bending and free vibration of functionally graded plates", *Steel Compos. Struct.*, **17**(1), 21-46.
- Koizumi, M. (1997). FGM Activities in Japan, *Composite: Part B*, **28**(1), 1-4.
- Samsam Shariat, B.A. and Eslami, M.R. (2005), "Effect of initial imperfection on thermal buckling of functionally graded plates", *J. Therm. Stress.*, **28**, 1183-1198.
- Sohn, K.J. and Kim, J.H. (2008), "Structural stability of functionally graded panels subjected to aero-thermal loads", *Compos. Struct.*, **82**, 317-325.
- Xiang, S. and Kang, G.W. (2013), "A nth-order shear deformation theory for the bending analysis on the functionally graded plates", *European J. Mech. A/Solids*, **37**, 336-343.
- Yamanouchi, M., Koizumi, M. and Shiota, I. (1990), *In Proc. First Int. Symp. Functionally Gradient Materials*, Sendai, Japan.
- Zenkour, A.M. and Sobhy, M. (2010), "Thermal buckling of various types of FGM sandwich plates", *Compos. Struct.*, **93**, 93-102.
- Zenkour, A.M. and Mashat, D.S. (2010), "Thermal buckling analysis of ceramic-metal functionally graded plates", *Nat. Sci.*, **2**, 968-978.

OP